Journal of Hydroscience and Hydraulic Engineering
Vol. 6, No. 2, December, 1988, pp.1-15

DELAY TIME MODEL FOR TANDEM CYLINDER VIBRATION

By

Charles W. Knisely

Department of Civil Engineering, Kyoto University, Kyoto, Japan

and

Hiroji Nakagawa

Department of Civil Engineering, Kyoto University, Kyoto, Japan

SYNOPSIS

Laboratory water channel experiments concerning the flow characteristics about two closely spaced (L/D = 1.5) tandem cylinders when the downstream cylinder undergoes forced oscillation are described. A hot-film probe was positioned on the shoulder of the downstream cylinder to estimate the delay time between cylinder motion and the switching of the high speed flow ("jet" flow) into the gap between the two cylinders. From measurement of this kinematic jet switching time, a delay time model for proximity galloping of tandem cylinders has been formulated. Solution of the equation of motion for the downstream cylinder employing this delay time model yielded results that were of the same order of magnitude as the laboratory results of Zdravkovich (19), but differences in detail were evident. Further refinement of the model and the numerical techniques are required before the amplitudes and frequencies of vibration can be predicted exactly. Experiments conducted after submission of the draft of the present paper (Knisely and Kawagoe (7)), in which the dynamic flow-induced lift force acting on the oscillating downstream cylinder was measured directly, indicate that the kinematic delay time measurements of the present experiment were of the correct order of magnitude, but did not accurately represent the behavior of delay time with increasing reduced velocity. New calculations using the revised delay time relationship are being undertaken and will be reported later.

INTRODUCTION

There are many different applications in which closely spaced tandem structures with circular cross-section are exposed to a mean velocity or current. In the area of hydraulics, pier supports (pilings), underwater cables, submerged pipeline bundles and the risers on an offshore oil platform are a few examples. Examples from wind engineering include closely spaced smokestacks, radio and television towers, distillation columns, storage tanks for oil or water, electrical power cables and closely spaced pipe racks. In the mechanical sciences, one immediately thinks of heat exchangers as an example of this type of geometry.

It is important to recognize that all of these diverse geometries in their often different environments are susceptible to flow-induced vibrations. In the following, the symbols L and T will be used to denote the center-to-center spacing in the Longitudinal (streamwise) and Transverse (cross-stream) directions, respectively; U signifies the freestream velocity; f_c is the frequency of cylinder vibration; t_c is the period of vibration ($t_c = 1/f_c$) and D represents the cylinder diameter. Tandem (implying small values of T/D) cylinder vibrations can be excited by a variety of mechanisms, depending mainly on the L/D ratio.

Cooper and Wardlaw (4) reported that when the streamwise spacing L/D>5, the downstream cylinder can undergo what is termed "wake galloping" or "wake flutter".

This type of vibration occurs when the reduced velocity, denoted by $U_R = U/f_cD$, exceeds a threshold value, known as the critical onset reduced velocity. The vibration of the downstream cylinder, characterized by elliptical orbits, is driven by the mean velocity gradients in the wake of the upstream cylinder.

A different type of oscillation can result when the streamwise cylinder spacing exceeds about six diameters (L/D>6). If the downstream structure has an eigenfrequency near the vortex shedding frequency of the upstream structure, the impinging von Karman vortices from the upstream structure can cause a resonant vibration of the downstream structure. This type of vibration is termed "resonant buffeting" and has been examined by Wong (18). As with all vortex-induced vibrations one must expect that resonant buffeting will occur only over a limited reduced velocity range.

King and Johns (5) investigated what they called "in-line proximity interaction" which can occur when the inter-cylinder spacing is less than six diameters (L/D<6) and the mass damping parameter $k_s<1.2$. The mass damping parameter is defined as $k_s = 2m_e\delta/\rho D^2$, where m_e is the modal mass, δ the logarithmic decrement of free vibration and ρ the fluid density. (The modal mass used in the water channel experiments of King and Johns (5) is defined as the integral of total mass (i.e., structural mass plus added mass) times the mode shape function evaluated over the entire cylinder length divided by the integral of the mode shape function over the wetted length of the cylinder.) This type of tandem cylinder interaction is usually limited to reduced velocities in the range $1.2<U_R<5$ and is characterized by cylinder motion in the flow direction.

"Cross-stream proximity interference galloping" or simply "interference galloping" has been discussed by many authors, among them Zdravkovich (19), Zdravkovich and Pridden (20), Ruscheweyh (14), Bokaian and Geoola (2, 3), Shiraishi et al (15) and most recently Matsumoto et al (10) and Knisely and Kawagoe (7). This type of cross-stream vibration generally occurs when the spacing ratio is less than three to four (L/D<3 to 4). Ruscheweyh (14) has shown that, although both cylinders may vibrate, the amplitude of the downstream cylinder is consistently larger than that of the upstream cylinder. Amplitudes of vibration are typically of the order of one diameter and vibrations can occur over a wide range of reduced velocities, nominally $15<U_R<100$ to 200, but both amplitude and reduced velocity range depend, of course, on the Scruton number (mass damping parameter). The remainder of the present paper will deal with this "interference galloping" phenomenon.

Ruscheweyh (14) measured the cross-stream response of the downstream cylinder of a tandem pair of finite length cylinders (H/D = 22) with a free end over the Reynolds number range $2 \times 10^3 \leq Re \leq 2 \times 10^4$ for various values of the Scruton number and streamwise cylinder spacing at four different angles of attack between the mean flow and the line of centers of the two cylinders. Ruscheweyh (14) also developed an "interference galloping criterion" by employing a quasi-steady analysis with an assumed constant phase shift between the cylinder motion and the quasi-steady lift force, which was assumed to be sinusoidal at the same frequency as cylinder motion. His prediction for the onset velocity, that is, the velocity where interference galloping begins, takes the following form:

$$U_{R_o} = \frac{U_o}{f_c\, D} = 3.54 \left[\frac{2M\,\delta}{\rho\, D^2} \right]^{1/2} \left[\frac{R/D}{-\partial C_L/\partial\beta\big|_\beta \,\sin\theta} \right]^{1/2} \tag{1}$$

Here, U_{R_o} is the reduced onset velocity; U_o the dimensional onset velocity; f_c the frequency of cylinder vibration; D the cylinder diameter; M the generalized mass per unit length; δ the logarithmic decrement (of free vibration); ρ the density of the flowing medium; R the intercylinder spacing along the line of centers; θ is the assumed phase lag of the lift relative to the cylinder displacement; and $\partial C_L/\partial\beta\big|_\beta$ is the slope of the lift coefficient curve evaluated at the angle β, where β is the angle between the line of centers and the direction of the oncoming mean flow.

The similarities and differences between his model and the classical galloping model were noted by Ruscheweyh. His model depends upon the square root of the

Scruton number and requires a <u>positive</u> slope for $\partial C_L/\partial\beta|_\beta$ (since sin θ is a negative quantity). Classical galloping theory, on the other hand, predicts a linear dependence of the onset velocity on the Scruton number and requires a negative slope of the lift coefficient curve. The expression $-\partial C_L/\partial\beta|_\beta \sin\theta > 0$ is termed the "interference galloping criterion."

Bokaian and Geoola (2, 3) measured the transverse amplitude response curves for both the downstream cylinder (Bokaian and Geoola (2)) and the upstream cylinder (Bokaian and Geoola (3)). The conditions in their experiments were as follows: spring mounted rigid body motion; $200 \leq Re \leq 6000$ (water flow); aspect ratio H/D, $18.63 \leq H/D \leq 37.25$. They reconfirmed the dependence of the onset velocity on the Scruton number. Further, their data roughly agreed with Ruscheweyh's (14) predicted square root dependence of the onset velocity on the separation distance. It should be noted that both Ruscheweyh (14) and Bokaian and Geoola (2) found an interaction between the mechanisms of interference galloping and classical vortex shedding, just as has been reported for the galloping of rectangular cross-section cylinders (see, for example, Wawzonek and Parkinson (17) and Bokaian and Geoola (1).

Ruscheweyh (14) avoided specifying the phase lag θ, by solving Eq. (1) for the parameter $-\partial C_L/\partial\beta|_\beta \sin\theta$ and employing an experimentally determined value for U_{R_o}. His model appears to give consistent results when used with his experimental data, but in order to apply the model to other situations more information concerning the value of θ is needed. Does θ depend on U_R, L/D and/or the amplitude of vibration A/D? The purpose of the present study is to obtain a crude estimate of θ, or, equivalently, of the delay time T_{js}.

The incorporation of a phase lag, or delay time, into a quasi-steady analysis is a method of accounting for the inertia of the oncoming flow and is a measure of the time required for the flow to react to a change in the cylinder position. This concept has appeared in the literature under the name "retardation effect" (Simpson and Flower (16)), "phase lag due to fluid inertia" (Lever and Weaver (8)) and "flow redistribution time" (Lever and Weaver (9)). Price and Paidoussis (12, 13) employed the retardation time of Simpson and Flower to calculate the elastic stability boundary of heat exchanger tube banks. They assumed a dimensionless delay time, $\tau_{js} = UT_{js}/D$, of order unity. To the authors' knowledge, no measurement of the delay time has been reported in the literature.

The mechanism which drives interference galloping is thought to be the periodic switching of high speed flow into and out of the gap between the two cylinders. When the two cylinders are aligned in the streamwise direction, there is only recirculating flow in the gap between the two cylinders and their common wake is symmetrical. In the aligned position the transverse displacement of the downstream cylinder, η, is defined to be zero. As the downstream cylinder moves away from the centerline, that is, $|\eta|>0$, it forces the wake to become unsymmetrical. At some critical transverse location, for a given L/D, the downstream cylinder presents a large enough flow obstruction to force the shear layer emanating from the upstream cylinder to bend into the gap between the two cylinders. The area of this gap is relatively small and the resultant gap flow has a high velocity. The induced pressure field acts to restore the cylinder to its inline arrangement, but the kinetic energy of the cylinder reaches a maximum just as it passes through the position corresponding to $\eta = 0$, and the cylinder's momentum carries the cylinder to a displaced position on the opposite side where the switching of high speed fluid, called "jet-switching" by Naudascher (11), occurs once again.

The physical significance of the phase shift in Ruscheweyh's (14) model, or, equivalently, a time delay between cylinder displacement and the equivalent quasi-steady loading, is presented in Fig. 1. In Fig. 1a the coordinate systems, (ξ,η) and (x,y), and the equilibrium position of the cylinder are defined. The coordinates (ξ,η) are fixed at the center of the upstream cylinder. The time mean position of the downstream cylinder, called the equilibrium position, is given by $\xi = L$ and $\eta = T$. The coordinates (x,y) have their origin at the equilibrium position of the downstream cylinder. Hence the two coordinate systems are related by $x = \xi - L$ and $y = \eta - T$. Note that for simplicity, the equilibrium position of the downstream cylinder in Fig. 1a and in the subsequent experiments is at the location just prior to the occurrence of "jet-switching". The η value corresponding to this location will be termed the "critical transverse displacement" since a slight displacement from this position would result in a significantly different flow pattern. This position is also given by β_{eq}, where $\beta_{eq} = \tan^{-1}(T/L)$. It is also assumed, again for simplicity, that the downstream cylinder undergoes harmonic oscillations as shown in Fig. 1b. To explain the phenomenon of interference galloping it is sufficient to consider vibration about the critical transverse displacement on one side of the wake only. Such an asymmetrical cylinder configuration would correspond to the oncoming flow approaching the cylinders at an angle of attack relative to the line of centers of the two cylinders. The force on the downstream cylinder is dominated by the gap flow. When the high speed "jet" flow occurs there is a negative lift force exerted on the downstream cylinder. When there is only recirculating flow, the net lift force is approximately zero.

Throughout the remainder of this paper, reference will be made to "static lift force" and "dynamic lift force." The first term, "static lift force," refers to the lift force acting on the downstream cylinder when it is displaced statically relative to the upstream cylinder, i.e., the velocity of the downstream cylinder remains zero for a long while before and during the measurement of the lift force. "Dynamic lift force" refers to the lift force acting on the cylinder as it is dynamically displaced relative to the upstream cylinder, that is, as it undergoes forced vibrations. The problem addressed in this paper is whether it is appropriate to model the dynamic lift force acting on the cylinder at time t as the static lift force acting on the cylinder if it were to be statically displaced a distance corresponding to the dynamic cylinder displacement at time $t-T_{js}$.

The static lift force is idealized as a step function as shown by the dashed line in Fig. 1c and d. The switching of the "jet" into and out of the gap, however, requires a finite amount of time due to the fluid inertia. The transverse dynamic lift force acting on the downstream cylinder is assumed to be similar to the idealized curve shown as the solid line in Fig. 1c. The finite time required for the jet to switch into and that required for it to switch out of

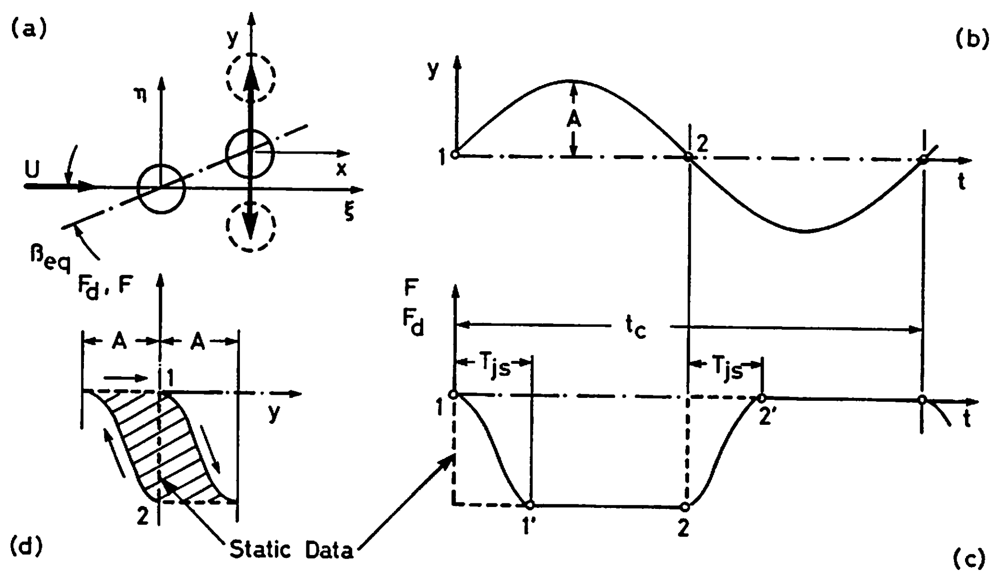

Fig. 1: Proposed mechanism for sustaining the oscillation of two closely spaced cylinders, after Naudascher (11) as depicted in Knisely (6)

the gap are assumed to be approximately equal and are both denoted by T_{js}. The significance of this delay time is evident in the force-displacement diagram in Fig. 1d. If the "jet switching" were instantaneous, the process would follow the line marked "static data" and the net area under the force-displacement curve would be exactly zero. The finite delay time results, however, in a closed loop which is traversed in a clockwise direction indicating energy transfer from the mean flow to the cylinder motion, thereby sustaining the cylinder vibration.

As previously mentioned, the experiments discussed in this paper were undertaken to find a crude value for the delay time. After presentation of the delay time measurements, a delay time model for cylinder interaction is formulated and initial results are presented. These initial results suggested that further refinement and better modelling of the delay time were required before the vibration model could accurately predict interference galloping, so no further calculations were carried out.

APPARATUS

Since the force on the downstream cylinder is dominated by the switching of the "jet" into and out of the gap, and since the instrumentation required for force measurement was unavailable, the experimental set-up shown in Fig. 2 was adopted. The downstream cylinder was forced to oscillate by means of a scotch yoke mechanism and the hot-film probe, mounted with the moving cylinder in a water flow, recorded the switching of the "jet" into and out of the gap. The placement of the hot-film probe was obviously crucial to the values obtained for delay time. Different probe locations would produce different delay times. After very careful observation using dye injection (see Photo 1 for a sample of the visualization), the position shown in Fig. 2, 43° from the forward stagnation point (in uniform flow), was chosen. The errors associated with this choice will be discussed in the section of this paper entitled "Results". Note that the hot-film probe was used only in a qualitative manner, so errors introduced by heat transfer to the nearby cylinder surface need not be accounted for.

Both cylinders were of diameter D = 5 cm. The equilibrium position of the downstream cylinder was approximately at the critical transverse displacement, just prior to the occurrence of "jet switching" into the gap. The value of L was 1.5D and T was 0.28D, resulting in an angle of β_{eq} = 10.6° (see Fig. 1) between their line of centers and the direction of the flow. The Reynolds number based on D and the freestream velocity in front of the cylinder pair was 8.5 x 10^3 for all

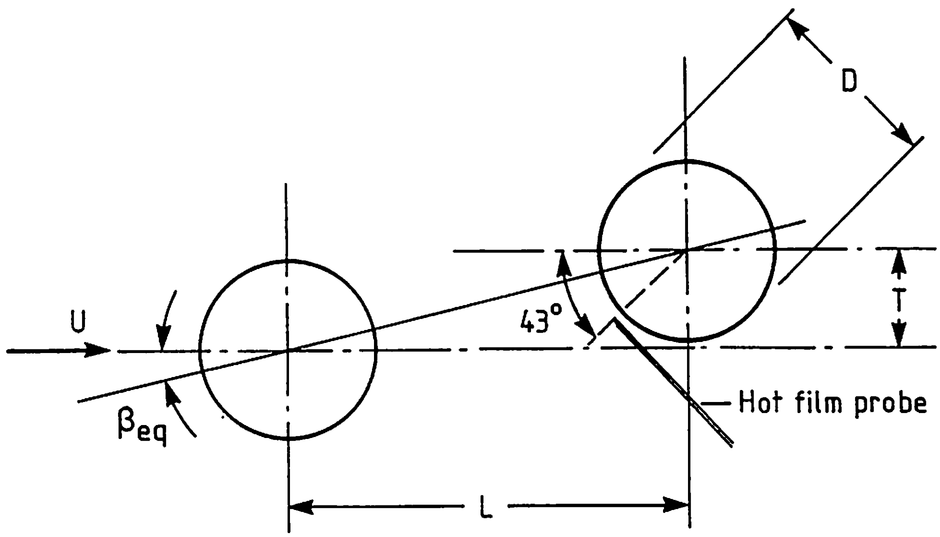

Fig.2: Experimental set-up for delay time measurement

experiments reported here. The frequency of <u>forced</u> vibration of the downstream cylinder was continuously variable, permitting reduced velocities, $U_R = U/(f_c D)$, over the range $5<U_R<50$. The amplitude of vibration could be varied continuously from 0 to 0.47D. The nominal water depth for the experiments was 20 cm, yielding a cylinder aspect ratio of 4. The channel was 50 cm wide, resulting in 10% blockage. No correction for blockage effects has been made. The corrections for blockage and for the short aspect ratio are, for a single cylinder, counterbalancing since blockage tends to increase the drag force, while a short aspect ratio tends to reduce it (Naudascher (11)). However, the small value of the aspect ratio and the high blockage must be regarded as possible sources of error when extrapolating to much larger aspect ratios in unbounded flow. All velocity measurements were made using a DISA 55M10 anemometer in conjunction with a DISA 55M25 linearizer and a conical hot film probe. The freestream streamwise velocity fluctuations were about 1% and the flow was uniform to within about one percent over the central 60% of the channel. Further details of the flow conditions can be found in Knisely (6).

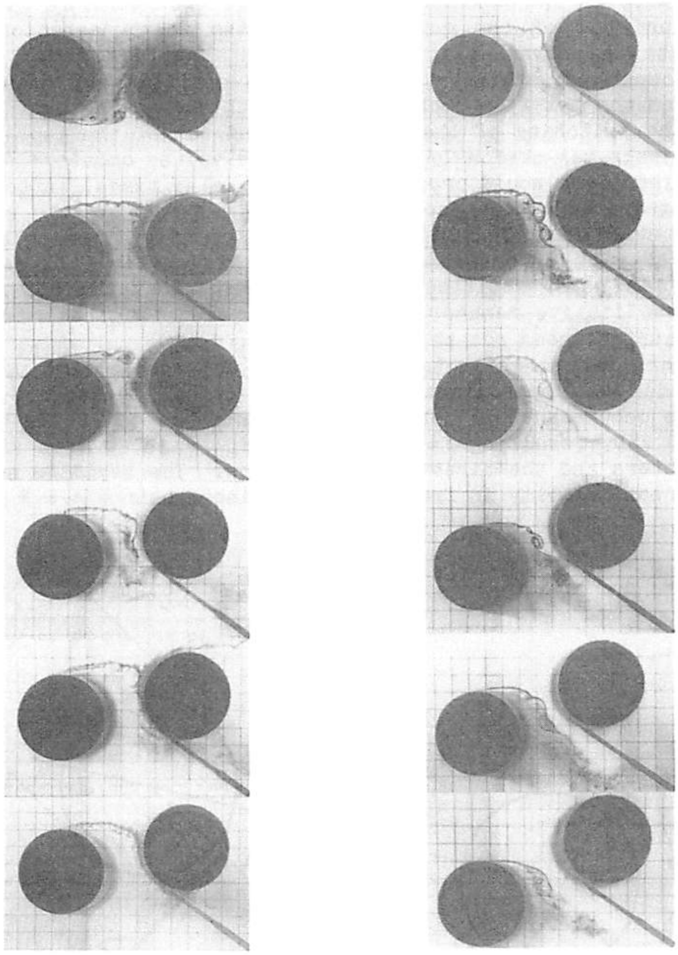

(a) $\eta/D=-0.184$ $y/D=-0.464$

(b) $\eta/D=0.187$ $y/D=-0.093$

(c) $\eta/D=0.216$ $y/D=-0.064$

(d) $\eta/D=0.266$ $y/D=-0.014$

(e) $\eta/D=0.272$ $y/D=-0.008$

(f) $\eta/D=0.307$ $y/D=0.027$

(g) $\eta/D=0.333$ $y/D=0.053$

(h) $\eta/D=0.383$ $y/D=0.103$

(i) $\eta/D=0.433$ $y/D=0.153$

(j) $\eta/D=0.504$ $y/D=0.224$

(k) $\eta/D=0.592$ $y/D=0.312$

(l) $\eta/D=0.750$ $y/D=0.470$

Photo 1: Flow visualization for various <u>static</u> displacements (cylinder velocity = 0) of the downstream cylinder. L/D = 1.5; Re = 8.5 x 10^3

Dynamic measurements were obtained using a Hewlett Packard 5451C Fourier Analyzer to phase average the velocity signal. The cylinder displacement signal, obtained from a variable inductance displacement transducer, was used as a phase reference. Normally 40 samples were used to determine the ensemble average. The contribution of the probe's own velocity to the output signal was checked and found to be negligible above a reduced velocity of 7. Again, details can be found in Knisely (6).

RESULTS

Flow Visualization

A better understanding of the mechanism of interference galloping can be gained by examining the flow visualization photographs in Photo 1. The downstream cylinder displacements shown in the photos are static displacements. The values of η/D give the absolute displacement of the cylinder from the symmetrical centerline of the flow, while the value y/D gives the displacement from the position where $\beta = 10.6^o$, which will be the equilibrium position of the cylinder in subsequent dynamic tests. (Thus, $y/D = \eta/D - T/D$, where $T/D = 0.28$.) In Photo 1a, the hot film probe, which is visible in all photos, is seen to be in the boundary layer of the downstream cylinder, which is exposed to the oncoming freestream since the shear layer from the upstream cylinder has been deflected into the gap. Reference will be made to this photo in the subsequent explanation of the small increase in velocity at extreme negative position of the cylinder.

For Photos 1b through 1e the dye filament emanating from the upstream cylinder appears to impact on the downstream cylinder. Upon impact, the dye filament splits, part of it proceeding downstream and part of it being deflected into the gap between the two cylinders. In Photo 1e and especially in Photo 1f, the dye filament diffuses much less into the gap, but rather maintains its identity and "adheres" to the cylinder surface in a manner similar to the well-known Coanda effect. It is in this range of y/D that the velocity signal shows a maximum value. The shear layer from the top side of the cylinder (in the photo) is apparently smoothly deflected along the surface of the downstream cylinder, producing a high local velocity and a low local static pressure. As the downstream cylinder is further displaced away from the centerline, the position of the downstream cylinder appears to force a more abrupt deflection of the shear layer, as shown in Photo 1g. With this more abrupt change in the shear layer deflection, the boundary layer on the downstream cylinder could conceivably separate before reaching the position of the hot film probe. This separation would account for the observed decrease in the static velocity signal over the range $0.05 \lesssim y/D \lesssim 0.15$. With further increases in y/D, the "jet-type" flow enters the gap more prominently. The angle that this jet makes with the horizontal mesh lines decreases continuously as the magnitude of y/D increases. This changing flow angle will be reflected in erroneous velocity measurements, since the sensitivity of the probe is direction dependent. Concurrent recordings of the hot film output for the statically displaced downstream cylinder are in complete agreement with these flow visualization observations. Sketches of visualization for $L/D = 3.0$ can be found in Shiraishi et al (15), showing similar behavior of the jet-type flow.

Ensemble Averaged Dynamic Data

A typical example of the ensemble averaged gap velocity and cylinder displacement signals when the downstream cylinder underwent forced vibration is given in Fig. 3. In this plot only, positive cylinder displacement is toward the bottom of the page. From Fig. 3 one can clearly see the delay time between the cylinder motion and the gap velocity. This delay time can be estimated by measuring directly from the time traces, as shown in Fig. 3, or by autocorrelating the two ensemble averaged time signals if one is content with a delay time averaged over all frequency components in the fluctuating velocity signal. Since even with 40 samples there were random fluctuations in the velocity signal, the delay time was defined to be the time from when the displacement crossed the zero level to when

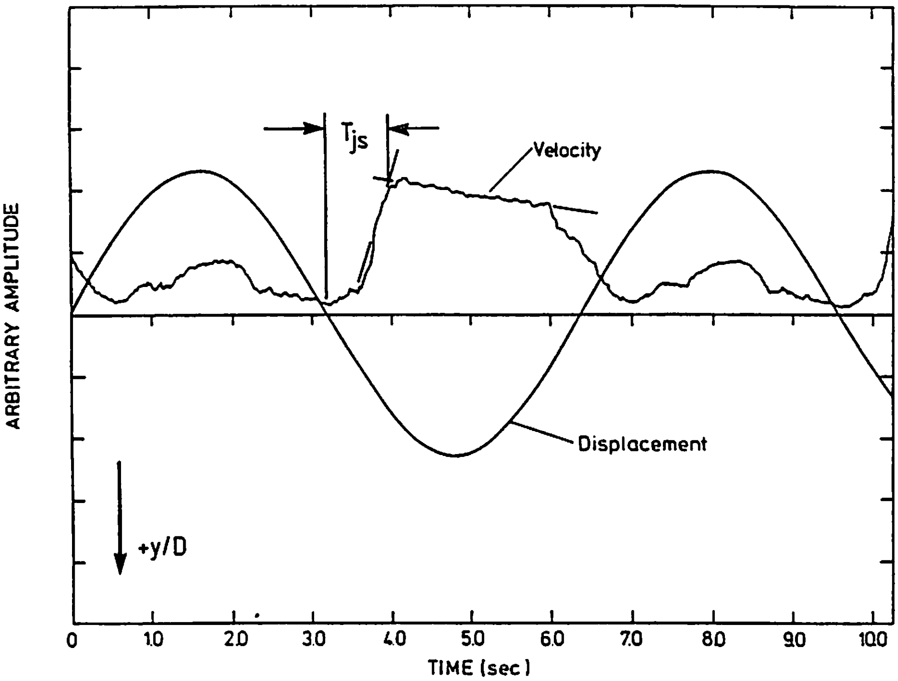

Fig. 3: Ensemble averaged dynamic gap velocity signal and cylinder displacement. $L/D = 1.5$, $T/D = 0.28$, $U_R = 16.5$, $A/D = 0.47$

the velocity signal reached the point defined by the intersection of the two lines approximating the mean slopes of the velocity signal, as shown in Fig. 3.

The results of the measurement of delay time required for the "jet" to switch into the gap for five different amplitudes of vibration and a range of reduced velocities is given in Fig. 4. Similar results were obtained for the time required for the jet to switch out of the gap. The data in Fig. 4 are well described by a linear correlation over the range of reduced velocities considered in the experiments. The correlations with a linear least squares curve fit are typically of the order of 90% or better. The worst fit and most scatter occurs when the amplitude of forced vibration is in the range 0.19D to 0.30D. Flow visualization results, discussed previously, revealed that in this amplitude range, the "jet" was formed by flow that first started around the outside of the downstream cylinder, but was subsequently forced to reverse direction and flow through the gap. The "jet flow" was attached to the downstream cylinder as it passed the forward stagnation point (in uniform flow), but conceivably separated before it passed the hot film probe located at 43°. It is believed that for this reason, the data for $A/D = 0.19$ and 0.30 are somewhat scattered. The dependence of the delay time on the details of the flow introduces considerable error. The delay time data presented here are only estimates and may vary as much as ±20%.

The delay time is clearly a function of the amplitude as well as the reduced velocity of the flow. Rigorously, the delay times presented in Fig. 4 are valid only for a Reynolds number (based on D and the freestream velocity) of 8.5×10^3.

To arrive at a single correlation curve, the least squares curve fits to the data (with correlations generally better than 90%) for the average delay times, $(T_{\text{switching in}} + T_{\text{switching out}})/2$, were re-plotted in many different forms, using Lotus 123 software to quickly plot the various combinations of parameters. The form that best correlated the data, and also made the most sense physically, is shown in Fig. 5, where the least squares curve fits to the delay time data are plotted as functions of the reduced velocity divided by the square root of the nondimensional amplitude of vibration. The quantity $U_R(A/D)^{-0.5}$ can also be written as $(U/\sqrt{D})(f_8^2 A)^{-0.5}$ and can be considered to represent the maximum non-dimensional cylinder acceleration. Note that the systematic variation of delay

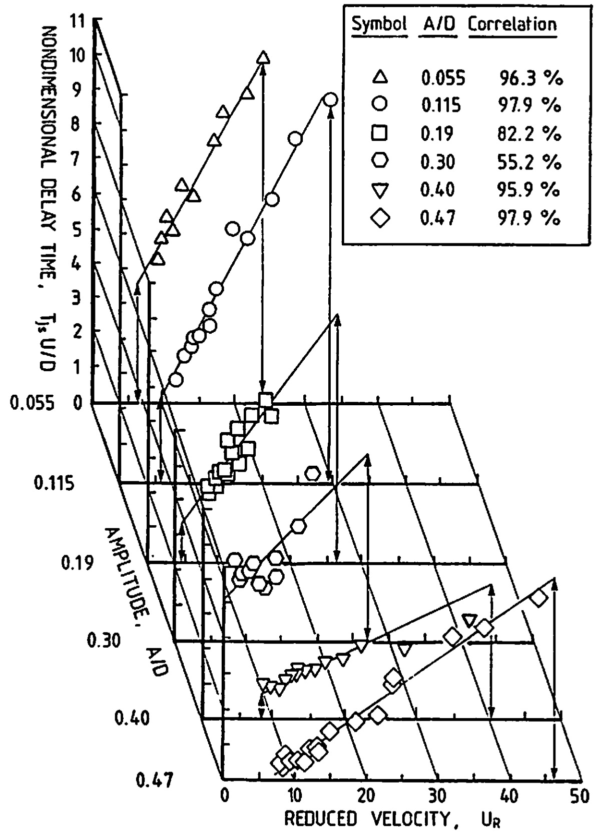

Fig. 4: Delay time for "jet switching" into the gap as a function of reduced velocity for A/D = 0.47, 0.40, 0.30, 0.21, 0.11 and 0.055

time with amplitude of vibration, found in Fig. 4, has disappeared in Fig. 5. The curves for A/D = 0.055, 0.3 and 0.47 are almost identical. The deviation of the other curves is most likely due to the details of the gap flow, that is, local separations. The errors involved in measuring the switching time in the manner employed here may be considerable, but the data do suggest that correlating the delay time with the parameter $U_R(A/D)^{-0.5}$ may be fruitful. The following non-dimensional correlation has been assumed, based on the data in Fig. 5:

$$\tau_{js} = T_{js}\ U/G = k_D\ (U/D)\ (f_c^2 A/D)^{-0.5} \tag{2}$$

where k_D is a nondimensional coefficient and the variable G has been substituted for D as the characteristic length. G is a measure of the approximate length of the free shear layer emanating from the upstream cylinder and is given by:

$$G = D\{(L/D)^2 + (T/D)^2 - T/D + 0.25\}^{0.5} \tag{3}$$

The value for the constant k_D will later be determined by a trial and error procedure so that the calculated results match the experimental laboratory results at a single point, i.e. at Re = 1×10^5. The test of the model then is whether the rest of the calculated data corresponds to the experimentally determined trends.

Employing Eq. (3) and recalling that $4\pi^2 f_c^2 A$ is equal to the maximum cylinder acceleration (for harmonic motion) one can arrive at the following correlation for the dimensional delay time:

$$T_{js} = k_D\ (G^2/D)^{0.5}\ |\ddot{y}_{max}/(4\pi^2)|^{-0.5} \qquad (4)$$

More refined experiments, conducted since the present analysis was undertaken and reported in Knisely and Kawagoe (7), suggest a different functional dependence of T_{js} on L/D. Since these more refined results were unknown at the time of the present analysis, however, the above correlation for T_D, Eq. (4), was employed in the delay time model of tandem cylinder interference galloping. Additional calculations using the more precise results will be undertaken later this year.

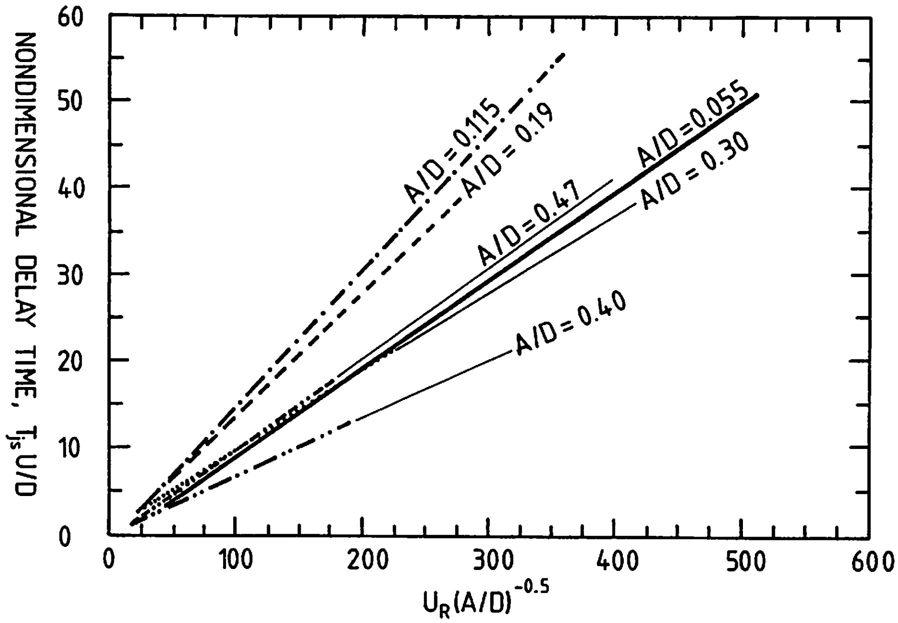

Fig. 5: Delay time vs. nondimensional acceleration parameter

EQUATION OF MOTION

The equation of motion for the downstream cylinder can be written as that of a simple forced oscillator, provided the cylinder vibrates as a rigid body, that is, the mode shape is given by $\psi = 1$. The forcing term on the right-hand side is the net flow-induced force per unit length in the y-direction. The equation of motion is

$$m\ddot{y} + c\dot{y} + ky = F_d(t) - C_D(0.5\rho\dot{y}^2 D) \qquad (5)$$

where it is assumed that the dynamic lift force, $F_d(t)$, can be given by the equivalent static force evaluated at a delay time T_{js}. Thus $F_d(t) = F(\xi,\eta^*)$, where F is the force corresponding to a static displacement and $\eta^* = \eta(t - T_{js})$.

Knowledge of the initial conditions and the static force distribution for static displacements, that is $F(\xi,\eta)$, coupled with the delay time model, Eq.(4), permits the solution of the equation of motion, Eq. (5), at least in theory.

NUMERICAL SOLUTION

The delay time inherent in the evaluation of L(t) causes significant problems if one attempts to solve Eq. (5). By assuming a starting cycle of undamped harmonic motion, the flow-induced force at negative times can be estimated for the start of the problem. The initial assumption is that the motion is nearly periodic, as was observed in the laboratory studies of Zdravkovich (19). The procedure is to neglect all damping and flow-induced forces and calculate one period of vibration of the undamped system. After one period of vibration, the cylinder is again at its original starting point with the same initial velocity and the same initial displacement. Rigorously this solution procedure is not valid, but as an engineering approximation for a process that is known to be almost periodic it may yield reasonable results.

The static lift distributions presented by Zdravkovich and Pridden (20) for Re = 6×10^4 were employed for the solution of the equation of motion. Analytical expressions were developed that closely resembled the static lift coefficient distribution, although these expressions did not match the empirical data exactly.

The second order problem was rewritten as two coupled first order equations and these were integrated using the Euler method. There is much room for refinement and optimization of the numerical techniques. The results presented here are intended to demonstrate that the delay time formulation does indeed lead to oscillatory behavior that follows the trends of the laboratory results of Zdravkovich (19).

The solution program was written in BASIC and calculations were carried out on a KAYPRO PC, an IBM compatible personal computer. The program solved the two first order equations by first assuming no damping and calculating the first cycle of cylinder motion. This first non-damped cycle was used to supply initial values for the static force evaluated at the delay time. Then the two first order equations were solved for time t using the static lift force corresponding to the position at time t-Tjs and finding the new position at $t+\Delta t$ by the Euler method. The maximum acceleration was evaluated at each half cycle and was used in Eq. (4) to evaluate the new value for delay time. The results are plotted as phase plane trajectories.

The calculated test cases were intended to emulate the experiments of Zdravkovich (19). In his paper, the exact mass, spring forces and damping are not presented; only the natural frequency and the damping factor are available. By making crude estimates concerning the density of the material he employed it was possible to examine a number of cases that should come close to his conditions, but no attempt was made to match the experimental data by adjusting the mass in the calculations.

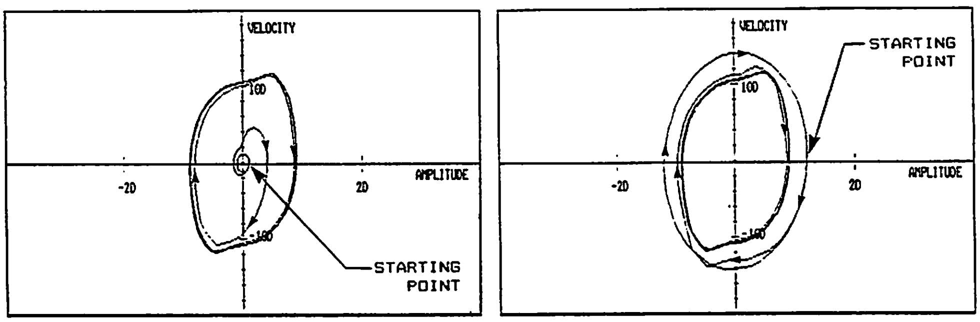

Fig. 6: Demonstration of independence of limit cycle from initial conditions. Calculations for m = 5 kg, c = 28 kg/s and k = 700 N/m

Unless otherwise noted, the results presented below are for an assumed mass per unit length of 2.0 kg, with a damping coefficient of 11.3 kg/s and a spring constant of 280 N/m. The delay time used in the calculations was determined from Eq. (4) as long as U_R was less than 80. For higher values of U_R, the delay time was assumed to remain constant at the value corresponding to U_R = 80. The value of k_D used in the calculations was 0.215.

There is considerable concern that the method of solution will lead to results which are a function of the initial conditions. Fig. 6 shows the limit cycle in the phase plane for two different initial conditions. In Fig. 6a the limit cycle is approached from below while in Fig. 6b the same limit cycle is approached from above. The results of calculations for variation with L/D and Reynolds number, neglecting any variation in k_D with Re, are compared with Zdravkovich's (19) laboratory data in Fig. 7. While the calculated results do not agree exactly in magnitude with the experimental results, the general trend with increasing Reynolds number is similar, while the trend with increasing L/D is the opposite of the experimental data. The lack of a sudden onset velocity in the numerical results is troubling, but may be due to the assumed form of the static lift coefficient distribution. Further, Zdravkovich indicated it was necessary to give the cylinder a significant initial displacement, whereas the numerical results showed limit cycle behavior for even the smallest displacement. Based on these preliminary findings, however, it would appear worthwhile to pursue this

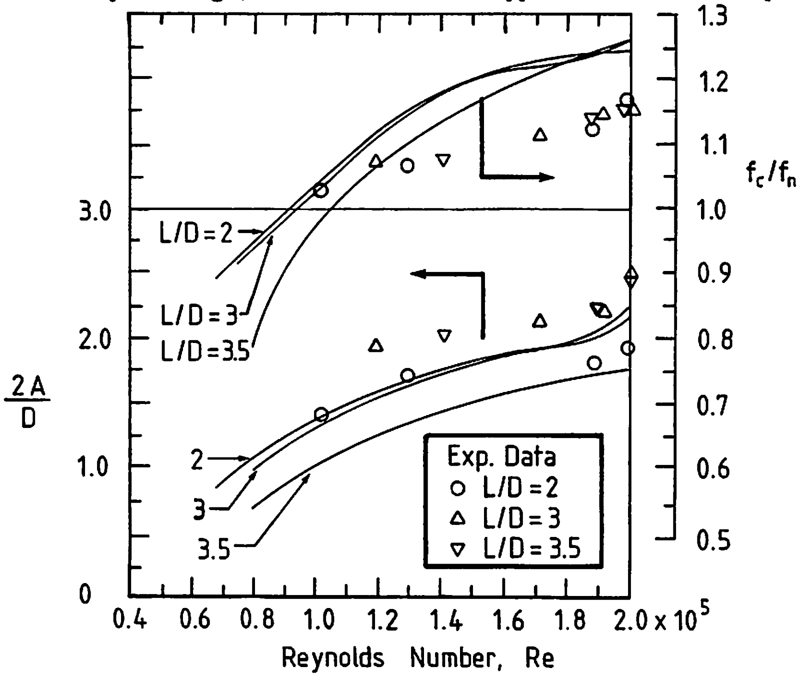

Fig. 7: Comparison of calculated results with experimental data from Zdravkovich (19). Upper curve is frequency ratio and lower curve reduced double amplitude

line of research. With necessary adjustments for variation in delay time and static lift coefficients with Reynolds number and numerical refinement, the proposed method may lead to an acceptable prediction of the proximity galloping of tandem cylinders.

CONCLUSION

From measurements of the kinematic jet switching time, a delay time model for interference galloping of tandem cylinders has been formulated. The preliminary solution of the equation of motion for the downstream cylinder employing this delay time model yielded results of the correct magnitude that agreed with the general trend of the laboratory results of Zdravkovich (19). Further refinement of the model and the numerical techniques are required before the amplitudes and frequencies of vibration can be predicted exactly.

To this end, recent measurements of the dynamic lift force as a function of cylinder position and reduced velocity were reported by Knisely and Kawagoe (7). Their results indicate that the kinematic delay time measurements of the present experiment were of the correct order of magnitude, but did not accurately represent the behavior of delay time with increasing reduced velocity. In the near future, the more precise correlation for delay time from Knisely and Kawagoe (7) will be incorporated into the mathematical model described here and new calculations performed.

REFERENCES

1. Bokaian, A. and F. Geoola: Hydroelastic instabilities of square cylinders, Journal of Sound and Vibration, Vol.92, pp.117-141, 1984.
2. Bokaian, A. and F. Geoola: Wake-induced galloping of two interfering circular cylinders, Journal of Fluid Mechanics, Vol.146, pp.383-415, 1984.
3. Bokaian, A. and F. Geoola: Proximity-induced galloping of two interfering circular cylinders, Journal of Fluid Mechanics, Vol.146, pp.417-449, 1984.
4. Cooper, K.R. and R.L. Wardlaw: Aeroelastic instabilities of wakes, Proceedings of the 3rd International Conference on Wind Effects on Buildings and Structures, Tokyo, pp.647-655, 1971.
5. King, R. and D.J. Johns: Wake interaction experiments in water, Journal of Sound and Vibration, Vol.45, pp.259-283, 1976.
6. Knisely, C.W.: Flow visualization and the kinematics of tandem cylinder interaction, Report SFB 210/E/15, Sonderforschungsbereich 210, University of Karlsruhe, Karlsruhe, W. Germany, 1985.
7. Knisely, C.W. and M. Kawagoe: Force-displacement measurements on closely spaced tandem cylinders, presented at the International Colloquium on Bluff Body Aerodynamics, Kyoto, 17-20 October 1988 and printed in Journal of Wind Engineering (Japan), No.37, pp.121-130, 1988.
8. Lever, J.H. and D.S. Weaver: A theoretical model for fluid-elastic instability in heat exchanger tube bundles, Journal of Pressure Vessel Technology, Vol.104, pp.147-158, 1982.
9. Lever, J.H. and D.S. Weaver: On the stability behavior of heat exchanger tube bundles: Part I - modified theoretical model, ASME Symposium on Flow-Induced Vibration, Vol.2: Vibration of Arrays of Cylinders in Cross Flow (ASME Book No. G00268), 1984.
10. Matsumoto, M., N. Shiraishi and H. Shirato: Aerodynamic instabilities of twin circular cylinders, presented at the International Colloquium on Bluff Body Aerodynamics, Kyoto, 17-20 October 1988 and printed in Journal of Wind Engineering (Japan), No.37, pp.131-140, 1988.
11. Naudascher, E.: <u>Engineering for Structures Subject to Flow-Induced Forces and Vibrations</u> (Notes from Intensive Course), 11-13 January, University of Karlsruhe, Karlsruhe, W. Germany, 1983.
12. Price, S.J. and M.P. Paidoussis: An improved mathematical model for the stability of cylinder rows subject to cross-flow, Journal of Sound and Vibration, Vol.97, pp.615-640, 1984.
13. Price, S.J. and M.P. Paidoussis: A theoretical investigation of the fluid elastic stability of a single flexible cylinder surrounded by rigid cylinders, ASME Symposium on Flow-Induced Vibration, Vol.2: Vibration of Arrays of Cylinders in Cross Flow (ASME Book No. G00268), 1984.
14. Ruscheweyh, H.: Aeroelastic interference effects between slender structures, Journal of Wind Engineering and Industrial Aerodynamics, Vol.14, pp.129-140, 1983.
15. Shiraishi, N., M. Matsumoto and H. Shirato: On aerodynamic instabilities of tandem structures, Journal of Wind Engineering and Industrial Aerodynamics, Vol.23, pp.437-447, 1986.
16. Simpson, A. and J.W. Flower: An improved mathematical model for the aeroelastic forces on tandem cylinders in motion with aeroelastic applications, Journal of Sound and Vibration, Vol.51, pp.183-217, 1977.
17. Wawzonek, M.A. and G.V. Parkinson: Combined effects of galloping instability and vortex resonance, Proceedings of the 5th International Conference on Wind Engineering, Ft, Collins, Colorado, Vol.2, pp.673-684, 1979.
18. Wong, H.Y.: Vortex-induced wake buffeting and its suppression, Journal of Wind Engineering and Industrial Aerodynamics, Vol.6, pp.49-57, 1980.
19. Zdravkovich, M.M.: Proceedings of the IUTAM/IAHR Symposium on Flow-Induced

Vibrations, Karlsruhe, Springer Verlag, Berlin, pp.631-639, 1974.
20. Zdravkovich, M.M. and D.L. Pridden: Interference between two cylinders; series of unexpected discontinuities, Journal of Wind Engineering and Industrial Aerodynamics, Vol.2, pp.255-270, 1977.

APPENDIX - NOTATION

The following symbols are used in this paper:

A	= amplitude of forced vibration;
c	= damping coefficient;
C_D	= drag coefficient;
C_L	= static lift coefficient;
D	= cylinder diameter;
f_c	= frequency of forced vibration;
$F(\xi,\eta)$	= static lift force distribution;
$F_d(t)$	= dynamic lift force;
G	= approximate shear layer length;
H	= length of cylinder;
k	= spring constant;
k_D	= delay time constant in Eq. (2);
k_s	= mass damping parameter of King and Johns (5);
L	= longitudinal (streamwise) center-to-center spacing between the two cylinders;
m	= mass per unit length;
m_e	= equivalent modal mass of King and Johns (5);
M	= generalized mass of Ruscheweyh (14);
$R = (L^2+T^2)^{1/2}$	= intercylinder spacing along the line of centers;
$Re = \rho UD/\mu$	= Reynolds number;
t_c	= period of forced vibration;
T	= transverse (cross-stream) center-to-center spacing between the two cylinders;
T_{js}	= dimensional jet switching time;
U	= freestream velocity in front of the cylinder pair;
U_o	= onset velocity for interference galloping;
$U_R = U/f_cD$	= reduced velocity;
$U_{R_o} = U_o/f_cD$	= reduced onset velocity;
x	= streamwise coordinate measured from the equilibrium position of downstream cylinder;
y	= transverse coordinate measured from the equilibrium position of downstream cylinder;
β	= angle of attack between oncoming flow and the line of centers;
$\beta_{eq} = \tan^{-1}(T/L)$	= β corresponding to the equilibrium position of the downstream cylinder;
δ	= logarithmic decrement of free vibration;

η = transverse coordinate measured from the center of upstream cylinder;

$\eta^* = \eta(t-T_{js})$ = transverse position of downstream cylinder for evaluation of equivalent static lift force;

θ = Ruscheweyh's (14) phase lag;

μ = fluid viscosity;

ξ = streamwise coordinate measured from the center of upstream cylinder;

ρ = fluid density;

$\tau_{js} = T_{js}U/G$ = nondimensional delay time; and

ψ = mode shape function.